Quantum-phase and information-entropy dynamics of a molecular system interacting with a two-mode squeezed coherent field

Masayoshi Nakano* and Kizashi Yamaguchi
Department of Chemistry, Graduate School of Science, Osaka University, Toyonaka, Osaka 560-0043, Japan
(Received 3 April 2001; published 14 August 2001)

We investigate the quantum dynamics for a molecular-state-model system interacting with a resonant two-mode squeezed coherent field, in which each mode is initially correlated. As an example, we consider a three-state molecular model, which mimics the electronic excited states of *trans*-octatetraene obtained by a full-configuration-interaction calculation using the Pariser-Parr-Pople Hamiltonian, interacting with a two-mode squeezed coherent field. For comparison, we also perform parallel studies, in which the initial fields are prepared in uncorrelated two-mode states, i.e., a two-mode coherent state and a two-mode thermal state. It is well known that the case of two-mode coherent field leads to the usual collapse-revival phenomena of the Rabi oscillations, while the case of a two-mode thermal state leads to an irregular evolution of them. Although the two-mode squeezed coherent field exhibits similar collapse-revival behavior to that for the two-mode coherent field, some differences are detected in the amplitudes and periods of collapse-revival oscillations. Further, the dynamics of off-diagonal molecular density matrices between the ground and second excited states for these two fields are found to be distinctively different from each other. Such attractive behavior is found to be closely associated with the two-mode photon-phase dynamics obtained by the Pegg-Barnett phase operator and the initial quasiprobability (Q function) distribution of photons. These differences in phase properties are also shown to significantly affect the dynamics of the information entropy for a molecule, i.e., molecular entropy, which represents the degree of entanglement between the molecule and photons.

DOI: 10.1103/PhysRevA.64.033415 PACS number(s): 42.50.Md, 33.80.−b, 33.15.−e, 42.50.Ct

I. INTRODUCTION

A subject of great interest in interdisciplinary research between quantum optics and quantum chemistry concerns the interaction of atoms and molecules with quantized (photon) fields [1–7]. The simplest model of such problems is the Jaynes-Cummings (JC) model [3–12], which describes the interaction between a two-state atom and a one-mode photon field. This model has an advantage in being exactly solved in the rotating-wave approximation (RWA). The result of this dynamics provides a purely quantum feature, e.g., collapse, quiescence, and revival behavior of the Rabi oscillations [13–20], which cannot be caused by conventional laser fields. Although these attractive features were predicted theoretically at first, recent experiments using Rydberg atoms in high-Q microwave cavities support some of these effects [21,22].

Various extensions of the JC model have attracted much attention over the last two decades. The quantum effects predicted in these models are used for the realization of optical communication [23] and laser cooling of atoms [24] and are further expected to be important in quantum information devices [25] in the future. Most of these studies have mainly focused on the quantum mechanical nature of photon dynamics. On the other hand, there have been few studies on the interactions among molecules and photon fields from the viewpoint of molecular science. In such studies, we need more general molecular models composed of arbitrary number of states and the non-RWA scheme, which can treat external fields with arbitrary frequencies. In previous studies [1–7], therefore, we performed a numerically exact treatment of such dynamics, which is referred to as electron-photon field dynamics (EPFD), and elucidated the relations among molecular properties and the dynamics of photon fields with various quantum statistics.

A recent direction of the extension is the consideration of the interaction between atoms and molecules and two-mode photon fields. In general, there are two types of two-mode fields, i.e., initially uncorrelated and correlated two-mode fields. Many studies on the dynamics of a three-state atom interacting with an uncorrelated two-mode field, e.g., two-mode thermal (chaotic) and two-mode coherent fields, have been carried out and have elucidated the feature of the dynamics from the viewpoint of the intermode field correlation [26,27]. There are also studies on the effect of initial intermode field correlations of two-mode squeezed vaccum [28] on the system dynamics [26]. The two-mode squeezed vacuum is a highly nonclassical state of the photon field in which the individual modes display random thermal fluctuations though a superposition of the modes exhibits a reduction in noise below the quantum limit [29]. For example, this feature is utilized in thermofield dynamics [30] and the physics of black holes [31]. The two-mode squeezed vacuum is also used for the generation of two-mode squeezed coherent fields [32–37] by the action of displacement operators.

The phase information on the photon field is known to be useful for understanding these dynamics. Recently, considerable progress in the study of the photon-phase properties of radiation fields has been made by Pegg and Barnett [38–40]. They introduced a set of formalisms defining a Hermitian phase operator, which allows us to calculate the phase distribution and various phase properties of one- and two-mode photon fields. For example, it was found that two-mode

*Corresponding author. Electronic address: mnaka@chem.sci.osaka-u.ac.jp

squeezed vacua exhibit elegant phase properties: they have random one-mode phases and the phase difference between the two modes is also random, while the phases lock so that their sum has a preferred value [40,41]. The method based on a quasiprobability, e.g., the Q function [42–44], distribution is also widely used due to its less abstract and more pictorial description of radiation fields. These quantities are also considered to be useful for our understanding of the quantum dynamics of matter-field-coupled systems. In previous studies [1–7], we elucidated the photon-phase dynamics for molecular model systems interacting with various one-mode photon fields and found that the features of splitting and colliding processes of the phase distribution remarkably depend on the number of molecular states, molecular transition quantities (transition energies and properties), the quantum statistical properties of the initial photon fields, and the detuning of the photon field. These results indicate that the photon-phase dynamics involves richer information on the time evolution of molecule-photon-coupled systems than the population dynamics. Although the population dynamics of atom-molecule systems under a two-mode squeezed vacuum has been investigated in detail [26], the photon-phase dynamics of atoms and molecules under two-mode squeezed fields (including a two-mode squeezed vacuum) has not been elucidated well yet.

Our motivation in this study is to investigate the relation of the dynamics of on- and off-diagonal molecular density matrices and the quantum statistics of the initially correlated two-mode photon field, i.e., two-mode squeezed coherent field. We consider a three-state molecular model, which mimics the electronic excited states of *trans*-octatetraene obtained by a full-configuration-interaction (FCI) calculation using the Pariser-Parr-Pople (PPP) Hamiltonian. As references, initially uncorrelated two-mode fields, i.e., two-mode coherent and two-mode thermal fields, are also considered. In addition to the dynamics of molecular populations, we elucidate the dynamics of two-mode photon-phase distributions (phase-sum and -difference distributions) using the Pegg-Barnett (PB) two-mode photon-phase operator. Another useful quantity characterizing quantum dynamics is the information entropy [45,46]. The molecule-field-coupled system generally evolves into an entangled state, where the molecule and field subsystems separately are in mixed states. Since the features of such entanglement are well described by the entropy of the subsystem, we analyze the features of the information entropy of the molecule (molecular entropy). The dynamical behavior of two-mode photon phases and molecular entropies for these two-mode fields are discussed in connection with the dynamics of molecular populations (diagonal molecular densities) and off-diagonal molecular densities, which represent the relative phase (coherency) between two electronic states.

We organize this paper as follows. We introduce our calculation method of a three-state molecule interacting with a two-mode photon field in Sec. II. In Sec. III, we explain a method for analysis using the two-mode PB phase distribution, Q function, and molecular entropy. In Sec. IV, we present a numerical study of the three-state molecule and two-mode field dynamics, concluding with a summary of our results in Sec. V.

II. DYNAMICS OF A MOLECULE-PHOTON-COUPLED SYSTEM

In this section, a Hamiltonian for a molecule interacting with a two-mode photon field and its calculation procedure (EPFD) are presented.

A. Hamiltonian for a coupled system composed of a molecule and a two-mode photon field

The Hamiltonian describing a molecular model with M states (M integer) in a two-mode photon field is constructed from $H_{\rm mol}$, the Hamilltonian of the unperturbed molecule system; $H_{\rm field}$, the Hamiltonian of the two-mode photon field; and $H_{\rm int}$, the interaction Hamiltonian:

$$H=H_{\rm mol}+H_{\rm field}+H_{\rm int}. \tag{1}$$

In the multipolar formalism under the dipole approximation, each part of the above Hamiltonian is expressed in the second-quantized representation as

$$H_{\rm mol}=\sum_{i}^{M} E_i a_i^{\dagger} a_i, \tag{2}$$

$$H_{\rm field}=\sum_{\lambda}^{2} \left(b_{\lambda}^{\dagger} b_{\lambda}+\frac{1}{2} \right) \hbar \omega_{\lambda}, \tag{3}$$

and

$$H_{\rm int}=\sum_{i,j}^{M} \sum_{\lambda}^{2} K_{\lambda} d_{ij} a_i^{\dagger} a_j (b_{\lambda}^{\dagger}+b_{\lambda}), \tag{4}$$

where

$$K_{\lambda} \equiv \left(\frac{\hbar \omega_{\lambda}}{2 \varepsilon_0 V} \right)^{1/2}. \tag{5}$$

In Eq. (2), E_i represents the energy of the molecular electronic state i, and $a_i^{\dagger}$ and a_i are, respectively, the creation and annihilation operators for the quantized electron field in the ith energy state. In Eq. (3), ω_{λ} indicates the frequency of photon mode λ, and $b_{\lambda}^{\dagger}$ and b_{λ} are the creation and annihilation operators for photon mode λ. The d_{ij} is the matrix element of the molecular dipole moment operator in the direction of the polarization of photon field. It is assumed that the polarization vectors of each mode coincide with each other. In Eq. (5), V is the volume of the cavity containing the photon field, and it is fixed to 10^7 Å^3 in this study.

The matrix elements of the above Hamiltonian are obtained using a triple Hilbert space spanned by the molecular states $\{|j\rangle\}$ ($j=1,2,...,M$) and the photon-number states of modes 1 and 2, i.e., $\{|n_1\rangle\}$ and $\{|n_2\rangle\}$ ($n_1,n_2=0,1,2,...,\infty$). Namely, the triple-Hilbert-space basis consists of the states $|j;n_1,n_2\rangle$ ($\equiv |j\rangle \otimes |n_1\rangle \otimes |n_2\rangle$). The matrix elements of the Hamiltonian, $H_{\rm mol}$, $H_{\rm field}$, and $H_{\rm int}$, are expressed as

$$\langle j;n_1,n_2|H_{\rm mol}|j';n_1',n_2'\rangle = E_j \delta_{jj'}\delta_{n_1 n_1'}\delta_{n_2 n_2'}, \tag{6}$$

$$\langle j;n_1,n_2|H_{\rm field}|j';n_1',n_2'\rangle = \sum_{\lambda}^{2}\left(n_\lambda+\frac{1}{2}\right)\hbar\omega_\lambda \delta_{jj'}\delta_{n_1 n_1'}\delta_{n_2 n_2'}, \tag{7}$$

and

$$\begin{aligned}\langle j;n_1,n_2|H_{\rm int}|j';n_1',n_2'\rangle &= d_{jj'}\{K_1(\sqrt{n_1'}\,\delta_{n_1,n_1'-1}+\sqrt{n_1'+1}\,\delta_{n_1,n_1'+1})\delta_{n_2,n_2'} \\ &\quad + K_2(\sqrt{n_2'}\,\delta_{n_2,n_2'-1}+\sqrt{n_2'+1}\,\delta_{n_2,n_2'+1})\delta_{n_1,n_1'}\}.\end{aligned} \tag{8}$$

B. Procedure of electron-photon field dynamics

The matrix elements of the time-evolution operator and the density matrix of the molecule-photon field system are provided. Using the eigenvalues $\{W(m)\}$ and eigenvectors $\{\chi(m)\}$ $(m=0,1,2,...)$ of the Hamiltonian [Eq. (1)], we obtain

$$H|\chi(m)\rangle = W(m)|\chi(m)\rangle, \tag{9}$$

where $m=0,1,2,\ldots,$ correspond to $(i;n_1,n_2)=(1;0,0),(1;0,1),(1;0,2),\ldots,$ respectively. Since this Hamiltonian is a Hermitian matrix, the eigenvectors $\{\chi(m)\}$ construct a complete orthonormal set:

$$\sum_m |\chi(m)\rangle\langle\chi(m)| = 1 \tag{10}$$

and

$$\langle\chi(n)|\chi(m)\rangle = \delta_{n,m}. \tag{11}$$

The solutions to the time-dependent Schrödinger equation

$$i\hbar\frac{\partial}{\partial t}|\Psi(t)\rangle = H|\Psi(t)\rangle \tag{12}$$

are represented as

$$|\Psi(t)\rangle = \sum_n e^{-iW(n)(t-t_0)/h}|\chi(n)\rangle \equiv U(t,t_0)|\Psi(t_0\rangle, \tag{13}$$

where the $U(t,t_0)$ is the time-evolution operator, which transforms the state at the initial time t_0 into the state at time t. The initial state vector $|\Psi(t_0)\rangle$ is expressed by

$$|\Psi(t_0)\rangle = \sum_n |\chi(n)\rangle. \tag{14}$$

The matrix element of the time-evolution operator is written as

$$\begin{aligned}&\langle j;n_1,n_2|U(t,t_0)|j';n_1',n_2'\rangle \\ &\quad\equiv U_{j,n_1,n_2;j',n_1',n_2'} \\ &\quad= \sum_m \langle j;n_1,n_2|\chi(m)\rangle\langle\chi(m)|j';n_1',n_2'\rangle e^{-iW(m)(t-t_0)/\hbar}.\end{aligned} \tag{15}$$

The elements of the density matrix are represented by

$$\begin{aligned}&\langle j;n_1,n_2|\rho(t)|j';n_1'n_2'\rangle \\ &\quad\equiv \rho_{j,n_1,n_2;j',n_1',n_2'}(t) \\ &\quad= \sum_{f,g}^{M}\sum_{\substack{m_1,m_2\\ m_1',m_2'}} U_{j,n_1,n_2;f,m_1,m_2}(t,t_0)\rho_{f,m_1,m_2;g,m_1',m_2'} \\ &\qquad\times(t_0)U^{\dagger}_{g,m_1',m_2';j',n_1',n_2'}(t,t_0).\end{aligned} \tag{16}$$

The procedure of EPFD is described as follows. First, we construct an initial density matrix $[\rho_{f,m_1,m_2;g,m_1',m_2'},(t_0)]$, which can be separated into the product of a molecular density matrix $[\rho^{\rm mol}_{f,g}(t_0)]$ and a two-mode photon density matrix $[\rho^{\rm 2phot}_{m_1,m_2;m_1',m_2'}(t_0)]$. The molecule is assumed to be in the ground state at the initial time. As the initial photon field, three types of two-mode photon fields, i.e., a two-mode coherent field (TC), a two-mode squeezed coherent field (TSC), and a two-mode thermal field (TT), are considered. The two-mode coherent (TC) and two-mode thermal (TT) fields are uncorrelated two-mode fields, so that their two-mode photon density matrices are constructed by a direct product of the density matrix concerning each one-mode field. The density matrix elements of a two-mode coherent field (TC) are expressed by

$$\rho^{\rm 2phot}_{m_1,m_2;m_1',m_2'} = \langle m_1,m_2|\beta_1,\beta_2\rangle\langle\beta_1,\beta_2|m_1',m_2'\rangle, \tag{17}$$

where the two-mode coherent state (TC) is

$$\begin{aligned}|\beta_1,\beta_2\rangle &= \exp\left[-\frac{1}{2}(|\beta_1|^2+|\beta_2|^2)\right] \\ &\quad\times\sum_{n_1}^{\infty}\sum_{n_2}^{\infty}\frac{\beta_1^{n_1}}{\sqrt{n_1!}}\frac{\beta_2^{n_2}}{\sqrt{n_2!}}|n_1,n_2\rangle.\end{aligned} \tag{18}$$

Here $\{\beta_\lambda\}$ is the eigenvalue of annihilation operator b_λ for photon mode λ with the eigenvector (coherent state) $\{|\beta_\lambda\rangle\}$. The density matrix elements of a two-mode thermal field (TT) are expressed as

$$\begin{aligned}\rho^{\rm 2phot}_{m_1,m_2;m_1',m_2'} &= \frac{\langle\hat{m}_1\rangle^{m_1}}{(1+\langle\hat{m}_1\rangle)^{m_1+1}}\frac{\langle\hat{m}_2\rangle^{m_2}}{(1+\langle\hat{m}_2\rangle)^{m_2+1}} \\ &\quad\times\delta_{m_1 m_1'}\delta_{m_2,m_2'},\end{aligned} \tag{19}$$

where $\hat{m}_\lambda$ is the photon-number operator defined by $\hat{m}_\lambda \equiv b_\lambda^\dagger b_\lambda$. It is noted that the thermal state has no off-diagonal elements, the feature of which indicates that the thermal state is a mixed state and has no definite phase relation between each photon-number state. In contrast to these fields, the two-mode squeezed coherent field (TSC) is a correlated two-mode field, so that it cannot be represented by the direct product of each one-mode density matrix. For two modes 1 and 2 with annihilation operators b_1 and b_2, the two-mode squeezed coherent field (TSC) $|\beta_1,\beta_2;\zeta\rangle$ is unitarily related to vacuum state $|0,0\rangle$ (the ground state of the two-mode field) by the action of two-mode squeezing operator $[\hat{S}_{12}(\zeta)]$ and two-mode displacement operator $[\hat{D}(\beta_1,\beta_2) \equiv \hat{D}(\beta_1)\hat{D}(\beta_2)]$ in the following manner [32–37]:

$$|\beta_1,\beta_2;\zeta\rangle = \hat{D}(\beta_1,\beta_2)\hat{S}_{12}(\zeta)|0;0\rangle, \tag{20}$$

where

$$\hat{D}(\beta_\lambda) = \exp(\beta_\lambda b_\lambda^\dagger - \beta_\lambda^* b_\lambda) \quad (\lambda = 1,2) \tag{21}$$

and

$$\hat{S}_{12}(\zeta) = \exp(\zeta^* b_1 b_2 - \zeta b_1^\dagger b_2^\dagger). \tag{22}$$

Here $\zeta = re^{i\varphi}$ is any complex number with modulus r and argument φ, which determine the squeezing intensity and direction of squeezing, respectively. It should be noted that $\hat{S}_{12}(\zeta)$ is not simply the direct product of two one-mode squeezing operators $[\hat{S}(\zeta) = \exp(-\zeta b^{+2}/2 + \zeta^* b^2/2)]$ for modes 1 and 2. Two-mode squeezing arises in models of two-photon nonlinear optics being associated with the non degenerate process, where pairs of photons are generated, one in each of modes 1 and 2, by the action of $b_1^\dagger b_2^\dagger$. It is also noted that the one-mode properties of each of the two-mode squeezed vacuum $|0,0;\zeta\rangle (\equiv S_{12}(\zeta)|0;0\rangle)$ are precisely those of a one-mode thermal state [34]. The relation among the average photon number of each mode, the displacement (β_λ) and squeezing (r) parameters, is represented by

$$\langle \hat{n}_\lambda \rangle - |\sinh r|^2 = |\beta_\lambda|^2 \geqslant 0 \quad (\lambda = 1,2). \tag{23}$$

The density matrix elements of the two-mode squeezed coherent field (TSC) are obtained by $\rho^{2\text{phot}}_{m_1,m_2;m_1',m_2'} = \langle m_1,m_2|\beta_1,\beta_2;\zeta\rangle\langle\beta_1,\beta_2;\zeta|m_1',m_2'\rangle$ using Eq. (20). Second, the density matrix elements $(\rho_{j,n_1,n_2;j',n_1',n_2'}(t))$ at time t are calculated using Eq. (16). Third, several reduced density matrix elements are calculated by

$$\rho^{\text{mol}}_{f,g}(t) = \sum_{m_1,m_2} \rho_{f,m_1,m_2;g,m_1,m_2}(t) \quad \text{(molecular density)}, \tag{24}$$

$$\rho^{2\text{phot}}_{m_1,m_2;m_1',m_2'}(t) = \sum_f \rho_{f,m_1,m_2;f,m_1',m_2'}(t)$$

(two-mode photon-field density), (25)

$$\rho^{1\text{phot}}_{m_1,m_1'}(t) = \sum_{m_2} \rho^{2\text{phot}}_{m_1,m_2;m_1',m_2}(t)$$

(one-mode photon-field density for mode 1), (26)

and

$$\rho^{1\text{phot}}_{m_2,m_2'}(t) = \sum_{m_1} \rho^{2\text{phot}}_{m_1,m_2;m_1,m_2'}(t)$$

(one-mode photon-field density for mode 2). (27)

Finally, various properties concerning the molecule and photons are calculated using these reduced density matrices.

III. PEGG-BARNETT PHASE OPERATOR, QUASIPROBABILITY (*Q* FUNCTION) DISTRIBUTION, AND INFORMATION ENTROPY

A. Pegg-Barnett phase operator

The phase properties of a one-mode photon field have been investigated since the first approach by Dirac [47]. Particularly, after Pegg and Barnett introduced a Hermitian phase operator [38] which overcomes several difficulties concerning the Susskind-Glogower phase operator [48], the phase properties of various photon fields and molecule-photon field coupled systems have been investigated [1–6,42–44]. They also extended their theory to analyze the phase properties of pairs of photon fields [40,41]. In this section, we briefly explain their two-mode PB phase operator for the analysis of the phase dynamics of the molecule-photon-coupled systems considered in this study.

In the Pegg-Barnett approach, all calculations concerning the phase properties are performed in an $(s+1)$-dimensional space spanned by $s+1$ orthonormal phase states, and the s value will be taken to be infinity after all expectation values have been calculated. The $s+1$ orthonormal phase states of a one-mode field are defined by

$$|\phi_m\rangle = \frac{1}{(s+1)^{1/2}} \sum_n^s e^{in\phi_m}|n\rangle, \tag{28}$$

where $\phi_m = \phi_0 + 2\pi m/(s+1)$ $(m = 0,1,2,...,s)$ and ϕ_0 is an arbitrary real number. In this study, s is taken to be 100 and we adopt $\phi_0 = -s\pi/(s+1)$ to locate the initial phase of a one-mode coherent photon field on the origin $(\phi = 0)$ of the phase axis defined in the region: $-\pi \leqslant \phi_m \leqslant \pi$. In the case of a two-mode field, these relations are satisfied for each mode field.

Pegg and Barnett defined the following Hermitian phase operator of mode λ to provide the eigenvalues $\{\phi_m^\lambda\}$ and the eigenstates $\{|\phi_m^\lambda\rangle\}$:

$$\hat{\phi}^\lambda = \sum_m^s \phi_m^\lambda |\phi_m^\lambda\rangle\langle\phi_m^\lambda|. \tag{29}$$

Based on this definition, we can calculate the expectation values of arbitrary continuous functions of the two-mode phase operator $[f(\hat{\phi}^1,\hat{\phi}^2)]$. By using the PB operator, the operator $f(\hat{\phi}^1,\hat{\phi}^2)$ can be defined as

$$f(\hat{\phi}^1,\hat{\phi}^2)=f\left(\sum_{m_1}^{s}\phi_{m_1}^1|\phi_{m_1}^1\rangle\langle\phi_{m_1}^1|,\sum_{m_2}^{s}\phi_{m_2}^2|\phi_{m_2}^2\rangle\langle\phi_{m_2}^2|\right)$$
$$=\sum_{m_1,m_2}^{s}f(\phi_{m_1}^1,\phi_{m_2}^2)|\phi_{m_1}^1\rangle|\phi_{m_2}^2\rangle\langle\phi_{m_1}^1|\langle\phi_{m_2}^2|. \tag{30}$$

The expectation values of $f(\hat{\phi}^1,\hat{\phi}^2)$ for arbitrary physical states $|\psi\rangle$ can be calculated by

$$\langle f(\hat{\phi}^1,\hat{\phi}^2)\rangle=\lim_{s\to\infty}\langle\psi|f(\hat{\phi}^1,\hat{\phi}^2)|\psi\rangle$$
$$=\lim_{s\to\infty}\sum_{m_1,m_2}^{s}f(\phi_{m_1}^1,\phi_{m_2}^2)P(\phi_{m_1}^1,\phi_{m_2}^2), \tag{31}$$

where $P(\phi_{m_1}^1,\phi_{m_2}^2)$ is the two-mode photon-phase distribution, which represents the joint probability density for phases $\phi_{m_1}^1$ and $\phi_{m_2}^2$. Using Eqs. (25) and (28), the two-mode phase distribution function can be expressed by

$$P(\phi_{m_1}^1,\phi_{m_2}^2)=\frac{1}{(s+1)^2}\sum_{\substack{n_1,n_2\\ n_1,n_2}}\rho_{n_1,n_2;n_1',n_2'}^{2\text{phot}}e^{i(n_1'-n_1)\phi_{n_1}^1}$$
$$\times e^{i(n_2'-n_2)\phi_{m_2}^2}. \tag{32}$$

The surface represented by $P(\phi_{m_1}^1,\phi_{m_2}^2)$ is 2π periodic along both ϕ^1 and ϕ^2 axes. Using Eqs. (31) and (32), we calculate various photon-phase properties for molecule-photon field coupled systems at time t. The phase-sum distribution $P(\phi_m^+)$ $[\equiv P(\phi_{m_1}^1+\phi_{m_2}^2)]$ is represented by

$$P(\phi_m^+)=\frac{1}{(s+1)}\sum_{n_1,n_2}\sum_{n_1'}\rho_{n_1',(n_1'-n_1+n_2);n_1,n_2}^{2\text{phot}}e^{i(n_1-n_1')\phi_m^+}. \tag{33}$$

The phase-difference distribution $P(\phi_m^-)$ $[\equiv P(\phi_{m_2}^2-\phi_{m_1}^1)]$ is represented by

$$P(\phi_m^-)=\frac{1}{(s+1)}\sum_{n_1,n_2}\sum_{n_1'}\rho_{n_1',(n_1-n_1'+n_2);n_1,n_2}^{2\text{phot}}e^{i(n_1'-n_1)\phi_m^-}. \tag{34}$$

We can also derive the one-mode photon-phase distribution $P(\phi_{m_\lambda}^\lambda)$ $(\lambda=1,2)$ using Eqs. (26) and (32) as follows:

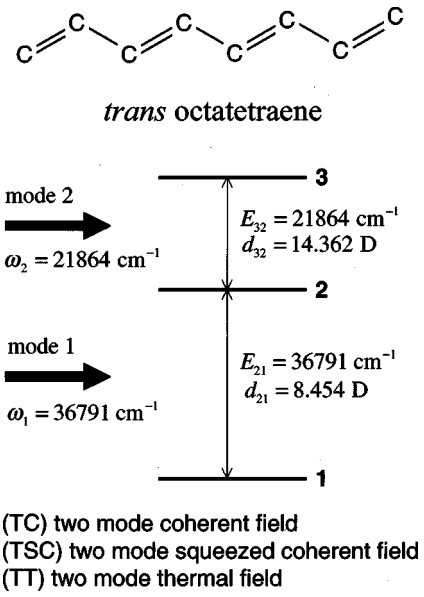

FIG. 1. Three-state molecular model (which mimics the electronic states of *trans*-octatetraene calculated by the PPP-FCI method [49]) interacting with a two-mode photon field. The ω_1 and ω_2 are frequencies which are resonant with energy intervals $E_{21}=36\,791\,\text{cm}^{-1}$ and $E_{32}=21864\,\text{cm}^{-1}$, respectively. The transition moments are $d_{21}=8.454D$ and $d_{32}=14.362D$. At the initial time, the molecule is assumed to be in the ground state, and we consider three types of photon fields, i.e., a two-mode coherent field (TC), a two-mode squeezed coherent field (TSC) with squeezing parameters $r=1.0$ and $\varphi=0$, and a two-mode thermal field (TT). The initial average photon number of each mode of these fields is 4.

$$P(\phi_{m_\lambda}^\lambda)=\frac{1}{s+1}\sum_{n_\lambda,n_\lambda'}\rho_{n_\lambda',n_\lambda}^{1\text{phot}}e^{i(n_\lambda-n_\lambda')\phi_{m_\lambda}^2}\quad(\lambda=1,2). \tag{35}$$

B. *Q* function

Another quantity characterizing photon-phase properties is the quasiprobability distribution, which is similar to a true probability distribution for the field amplitude. Namely, the moments of products b and $b^\dagger$ can be calculated by evaluating an integral weighted by the quasiprobability distribution. The Q function for a one-mode field is defined by

$$Q(\beta,t)=\frac{1}{\pi}\langle\beta|\rho^{1\text{phot}}(t)|\beta\rangle$$
$$=\frac{1}{\pi}e^{-|\beta|^2}\sum_{n,n'}\frac{\beta^{*n}\beta^{n'}}{\sqrt{n!n'!}}\rho_{n,n'}^{1\text{phot}}(t), \tag{36}$$

where $|\beta\rangle$ is a one-mode coherent state, β is its complex amplitude, and n is a photon number.

C. Information entropy of a molecule

The information entropy obtained form the reduced density matrix of the subsystem represents the degree of the lack of information (correlation) due to the reduction from the

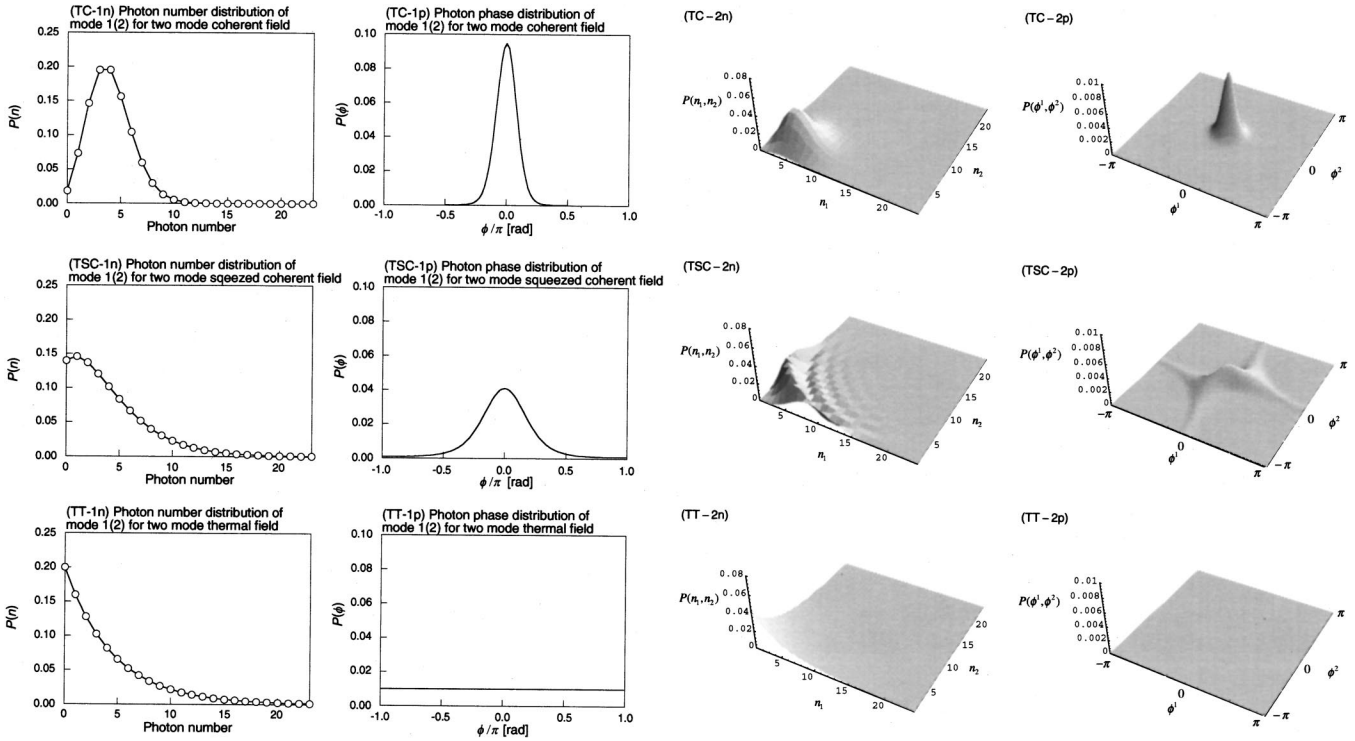

FIG. 2. One- and two-mode photon-number distributions $[P(n)$ and $P(n_1,n_2)]$ for a two-mode coherent field $[(\text{TC-}1n)$ and $(\text{TC-}2n)]$, a two-mode squeezed coherent field $[(\text{TSC-}1n)$ and $(\text{TSC-}2n)]$ and a two-mode thermal field $[(\text{TT-}1n)$ and $(\text{TT-}2n)]$. One- and two-mode photon-phase distributions $[P(\phi)$ and $P(\phi^1,\phi^2)]$ (based on the Pegg-Barnett phase operator) for these fields are also shown in $[\text{TC-}1(2)p]$, $[\text{TSC-}1(2)p]$, and $[\text{TT-}1(2)p]$, respectively.

total density matrix to the reduced density matrix for the subsystem. As an example, the information entropy of molecule (molecular entropy) is calculated by

$$S^{\text{mol}} = -\text{Tr}(\rho^{\text{mol}} \ln \rho^{\text{mol}}) = -\sum_j^M \rho_{jj}^{\text{mol}'} \ln(\rho_{jj}^{\text{mol}'}), \quad (37)$$

where $\rho^{\text{mol}'}$ is a diagonalized molecular reduced density matrix. For a pure state, $S^{\text{mol}}=0$, while, for a mixed state, $S^{\text{mol}}>0$. Namely, the time evolution of the molecular entropy reflects the time evolution of the degree of entanglement between the molecule and the two-mode photon field. The larger the entropy, the greater the entanglement.

IV. QUANTUM DYNAMICS OF A THREE-STATE MOLECULAR SYSTEM INTERACTING WITH AN INITIALLY TWO-MODE PHOTON FIELD

A. Molecular population dynamics

We consider a three-state molecular system (see Fig. 1) which mimics the electronic excited states of *trans*-octatetraene, which is known to be a typical π-conjugated linear-chain system. It is found from a PPP-FCI calculation [49] that the energy intervals are $E_{21}(\equiv E_2-E_1) = 36\,791\ \text{cm}^{-1}$ and $E_{32}(\equiv E_3-E_2) = 21\,864\ \text{cm}^{-1}$, and the transition moments in the chain-length direction of *trans*-octateraene are $d_{21}=8.454D$ and $d_{32}=14.362D$. We consider the frequencies ($\omega_1 = 36\,791\ \text{cm}^{-1}$ and $\omega_2 = 21\,864\ \text{cm}^{-1}$) of an initially two-mode photon field, which are resonant with E_{21} and E_{32}, respectively. The average photon number of each mode is fixed to $\langle \hat{n}_1 \rangle = \langle \hat{n}_2 \rangle = 4$. The squeezing parameters of the two-mode squeezed coherent field (TSC) are $r=1.0$ and $\varphi=0$. It is noted that the one-mode photon-phase and one-mode photon-number distributions for the two-modes of these fields are identical with each other at the initial time, respectively: $P(n_1)=P(n_2) \equiv P(n)$ and $P(\phi^1_{m_1})=P(\phi^2_{m_2}) \equiv P(\phi_m)$ at $t=0$. Figure 2 shows the one-mode photon-number distributions $P(n)$ $[(\text{TC-}n), (\text{TSC-}n)$, and $(\text{TT-}n)]$ and two-mode photon-number distributions $P(n_1,n_2)$ $[(\text{TC-}2n), (\text{TSC-}2n)$, and $(\text{TT-}2n)]$ at $t=0$. As is well known, the distributions $P(n)$ for the two-mode coherent (TC) and two-mode thermal (TT) fields exhibit Poisson and Bose-Einstein distributions, respectively. The distribution $P(n)$ of the two-mode squeezed coherent field (TSC) show an intermediate distribution between that for the two-mode coherent field (TC) and that for the two-mode thermal field (TT). This can be understood by the fact that the squeezing intensity (r) for the two-mode squeezed coherent field (TSC) takes an intermediate value ($r=1.0$) between that ($r=0.0$) for the two-mode coherent field (TC) and that $[r=\sinh^{-1}(\sqrt{\langle \hat{n}_\lambda \rangle}) \approx 1.443\,635\,475$; see Eq. (23)] for the two-mode squeezed vacuum, whose one-mode distribution coincides with that for the two-mode thermal field (TT) with the same average photon number. The distributions $P(n_1,n_2)$ represent the feature of correlation between the two modes of these fields: the $P(n_1,n_2)$ for the two-mode coherent (TC) and two-mode thermal (TT) fields are constructed by $P(n_1) \otimes P(n_2)$, while the $P(n_1,n_2)$ for the

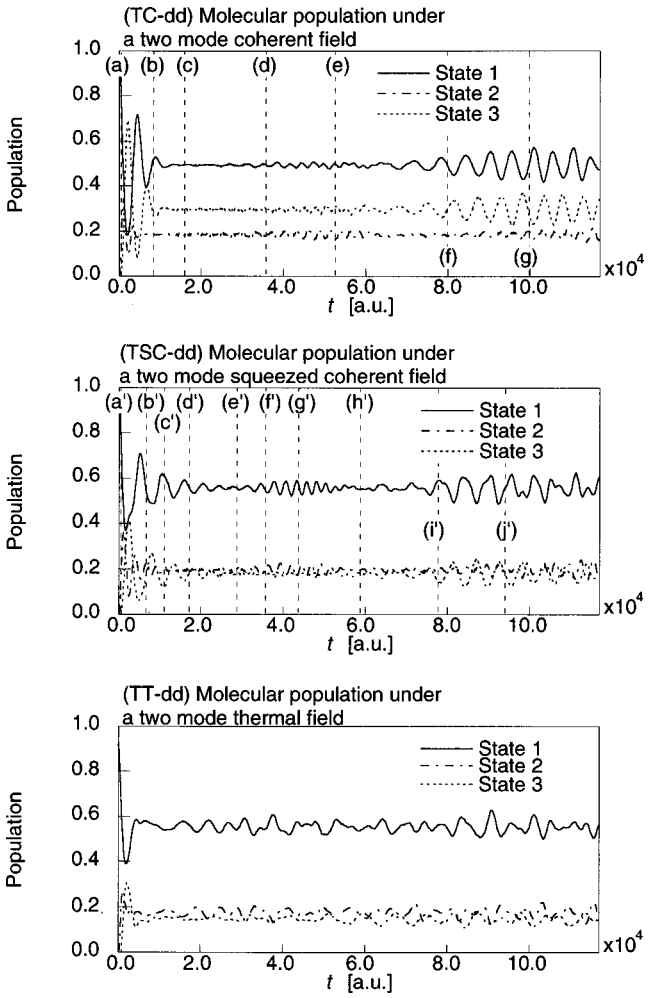

FIG. 3. Time evolution of the population of each state of the molecule (Fig. 1) for the two-mode coherent field (TC), two-mode squeezed coherent field (TSC), and two-mode thermal field (TT) is shown in (TT-*dd*), (TSC-*dd*), and (TT-*dd*), respectively.

two-mode squeezed coherent fields (TSC) is not constructed by $P(n_1)\otimes P(n_2)$. It is also found that the distribution $P(n_1,n_2)$ for the two-mode squeezed coherent field (TSC) exhibits oscillations which are similar to those in the high-number tail of the photon-number distribution for a one-mode squeezed field. Each peak of the oscillation for $P(n_1,n_2)$ appears with parabolic shapes which are symmetric about the diagonal line $n_1=n_2$. The features of such oscillations are known to be explained by the interference in phase space [37].

The molecular populations of each state [the ground state (1), the first excited state (2), and the second excitetd state (3)] for the two-mode coherent (TC), two-mode squeezed coherent (TSC), and two-mode thermal (TT) fields are shown in Fig. 3 [(TC-*dd*), (TCS-*dd*), and (TT-*dd*), respectively]. As observed in the previous study [26], the two-mode coherent field (TC) exhibits damped oscillations, i.e., collapses, and amplified oscillations, i.e., revivals, while the collapse-revival behavior for the two-mode thermal field (TT) is shown to be instantly damped and then the oscillations with small amplitudes are shown to continue at later times. The mechanism of the collapse-revival phenomena for a coherent field has been analyzed well and is found to originate in the dephasing and rephasing among the Rabi oscillations with slightly different frequencies [13–20]. It is noted that there are two types of revival-collapse regions for the two-mode coherent field (TC), one of which exhibits larger amplitudes than the other. By comparison of the molecular population of each state ($\rho_{1,1}^{\mathrm{mol}}$, $\rho_{2,2}^{\mathrm{mol}}$, and $\rho_{3,3}^{\mathrm{mol}}$), these two types of revival-collapse regions are found to be predominantly caused by one- and two-photon processes, respectively. Similar behaviors are observed in a three-state molecule under a one-photon resonant coherent field [1] and in a dimer composed of identical two-state molecules under a one-photon coherent field [6]. Similarly, in the previous study [26], the rapid reduction of the collapse-revival behavior is observed for the two-mode thermal field (TT). This behavior is found to be caused by the fact that there are no definite relative phase relations among the Rabi oscillations generated by the thermal field, which is a mixed state composed of various phase components. For the two-mode squeezed coherent field (TSC), we find that the Rabi oscillations are fairly similar to those of the two-mode coherent field (TC), although the squeezing intensity (r) for the two-mode squeezed coherent field (TSC) considered here takes an intermediate value between that for the two-mode coherent (TC) and that for the two-mode squeezed vacuum as mentioned above. The two types of collapse-revival behaviors are also detected in the two-mode squeezed coherent field (TSC), while the first collapse time (the time taken for the envelope to collapse to zero) and the starting time of the first revival for the two-mode squeezed coherent field (TSC) are longer and earlier than those for the two-mode coherent field (TC), respectively. Also, the difference in the amplitudes between the first and second revival-collapse regions for the two-mode squeezed coherent field (TSC) is found to be more reduced than that for the two-mode coherent field (TC) case. For the two-mode coherent field (TC), the averaged molecular population of state 3 is larger than that of state 2, while for the two-mode squeezed coherent field (TSC) the averaged molecular populations of states 2 and 3 are shown to be similar to each other. Such features indicate that the degree of the contribution of the two-photon process for the two-mode squeezed coherent field (TSC) is smaller than that for the two-mode coherent field (TC). These attractive behaviors of molecular populations are analyzed using the photon-phase and off-diagonal molecular density dynamics for the cases of these fields.

B. Initial photon-phase distributions

Before examining the phase and off-diagonal molecular dynamics of the molecule-photon-coupled systems, we investigate the features of the one- and two-mode photon-phase distributions [$P(\phi)$ and $P(\phi^1,\phi^2)$, respectively] of the two-mode coherent (TC), two-mode squeezed coherent (TSC), and two-mode thermal (TT) fields (see Fig. 2 [(TC-1p), (TSC-1p), and (TT-1p)] for $P(\phi)$ and Fig. 2 [(TC-2p), (TSC-2p), and (TT-2p)] for $P(\phi^1,\phi^2)$). The distribution $P(\phi)$ of the two-mode coherent field (TC) ex-

hibits a single sharp peak around $\phi=0$, which is caused by the fact that the coherent field is a state with the minimum Heisenberg uncertainty relation between orthogonal quadratures: the variance of each quadrature ($\Delta x_l^2=\Delta x_{l+\pi/2}^2$, l an arbitrary number) is equal to 1/4, while the two-mode thermal field (TT) exhibits a uniform one-mode photon distribution $P(\phi)$ since the thermal field is a mixed state composed of random phase components. The distributions $P(\phi^1,\phi^2)$ for the two-mode coherent (TC) and two-mode thermal (TT) fields are constructed by the direct products of their one-mode photon distributions $P(\phi)$ since these two fields are uncorrelated two-mode fields. On the other hand, the distribution $P(\phi)$ for the two-mode squeezed coherent field (TSC) is shown to possess a broader phase distribution peak than that for the two-mode coherent field (TC). It is well known that further squeezing causes more broadening of a phase peak and eventually leads to complete agreement between the distribution $P(\phi)$ of the two-mode squeezed vacuum and that of the thermal field. Therefore, we can say that the distribution $P(\phi)$ of the two-mode squeezed coherent field (TSC) exhibits an intermediate feature between the distribution $P(\phi)$ of the coherent and that of the thermal fields. However, the distribution $P(\phi^1,\phi^2)$ for the two-mode squeezed coherent field (TSC) is found to have more complicated structures in contrast to the uncorrelated two-mode fields, i.e., the two-mode coherent (TC) and two-mode thermal (TT) fields. The distribution $P(\phi^1,\phi^2)$ of the two-mode squeezed coherent (TSC) field is found to be generated by extensions of the phase distribution of the two-mode coherent field (TC) along the two directions, which are parallel to the lines $\phi^2=\phi^1$ and $\phi^2=-\phi^1$, respectively. It is noted that the two stretched leg regions in the direction of the line $\phi^2=-\phi^1$ approach the lines $\phi^2=-\phi^1-\pi$ and $\phi^2=-\phi^1+\pi$, respectively, as the squeezing intensity (r) increases. This feature suggests that the photon-phase-sum distribution for the two-mode squeezed vacuum, which has a limitting squeezing intensity [$r=\sinh^{-1}\sqrt{\langle\hat{n}\rangle}$: see Eq. (23)], exhibits a single peak around $\phi^1+\phi^2=\pm\pi$.

C. Dynamics of photon-phase-sum and -difference distributions

We next investigate the dynamics of two-mode photon-phase distributions, i.e., photon-phase-sum $P(\phi^+)$ [$\equiv P(\phi^1+\phi^2)$] and photon-phase-difference $P(\phi^-)$ [$\equiv P(\phi^2-\phi^1)$] distributions. Figure 4 shows these distributions at times [(a)–(g) for the two-mode coherent field (TC) and (a′)–(j′) for the two-mode squeezed coherent field (TSC)] represented by dotted lines shown in Fig. 3. The distribution $P(\phi^+)$ corresponds to the sum of pure phase parts, whereas the distribution $P(\phi^-)$ includes the phase $[(\omega_2-\omega_1)t]$ of the free field since the time t is taken as $2\pi m/(\omega_1+\omega_2)$ ($m=0,1,2,...$) in this study. However, the changes in the shape of the distribution $P(\phi^-)$ can be investigated by considering its 2π periodicity, although the phase origin moves at each time due to the contribution of the free field. The distributions $P(\phi^+)$ and $P(\phi^-)$ for the two-mode thermal state (TT) are not shown since they are uniform and constant at all times as seen from its definition.

Before analyzing the two-mode photon-phase dynamics, we briefly explain the relation between the photon-phase distribution dynamics and the collapse-revival behavior of the Rabi oscillations in the case of a molecule coupled with a one-mode photon field [1–5,42,43]. It was found that splitting and colliding processes in the phase distribution occur in the case of a coherent field. In the early-time region, a single phase peak around $\phi=0$ is split as the collapse behavior of the molecular population proceeds. In the next-time region, the split peaks move in mutually opposite directions, and then these two peaks collide at $\phi=\pm\pi$. As a result of the 2π periodicity of the phase space, after the collision at $\phi=\pm\pi$, each peak which passed $\phi=+\pi$ and $\phi=-\pi$ appears again from the side of $\phi=-\pi$ and $\phi=\pi$, respectively, and then these two peaks move to $\phi=0$. In such a manner, the splitting and colliding of peaks are repeated. Throughout these processes, the peaks in the phase distribution gradually decrease and cause a broadening, the feature of which is evidence of the uncertainty relation between a photon phase and a photon number. The collapse and revival behaviors in the molecular population correspond to the splitting and colliding processes in the photon-phase distribution, respectively. This correspondence is interpreted as follows. In the coherent photon field, the splitting process in the photon-phase distribution first causes an increase in the ability to destroy the coherence between the molecular states and then causes a gradual decrease in that ability due to the large splitting of the photon phase (approaching $\phi=\pm\pi/2$). In contrast, the colliding process causes a gradual increase and successive decrease in that ability. Such variations in the coherence between the molecular states cause the collapse-revival behavior of the molecular population. However, the splitting and colliding are not completely achieved in the larger-time region, so that the increase and decrease in that ability become unclear as the time proceeds. These changes are reflected in the dynamics of the molecular entropy and off-diagonal molecular density matrix [1–7].

First, we consider the relation among the dynamics of the ground-state molecular population and that of distributions $P(\phi^+)$ and $P(\phi^-)$ of the two-mode coherent field (TC) case. The initial $P(\phi^+)$ and $P(\phi^-)$ distributions for the two-mode coherent field (TC) provide an identical single peak around $\phi^+=\phi^-=0$. This is evident from the distribution $P(\phi_1,\phi_2)$ for the two-mode coherent field (TC) shown in Fig. 2 [TC-2p]. It is noted that the distributions $P(\phi^+)$ and $P(\phi^-)$ correspond to the sum of the distribution $P(\phi_1,\phi_2)$ along direction parallel to the lines $\phi^2=-\phi^1$ and $\phi^2=\phi^1$, respectively. The first collapse behavior at times (a), (b), and (c) for the two-mode coherent field (TC) (see Fig. 3) is found to correspond to the split into three peaks and the subsequent moving of the side peaks (in mutually opposite directions) of the distribution $P(\phi^+)$ (see Fig. 4 [(TC)(a)–(c)]). This is similar to the behavior of a three-state molecule under a one-photon coherent field [1,2]. On the other hand, the distribution $P(\phi^-)$ shows no split of the peak until time (c). This is understood by the fact that the phase sum ϕ^+ ($\equiv\phi^1+\phi^2$) has a larger frequency than the phase difference ϕ^- ($\equiv\phi^2-\phi^1$). At time (c) for the two-mode coherent field (TC), although the distribution $P(\phi^-)$

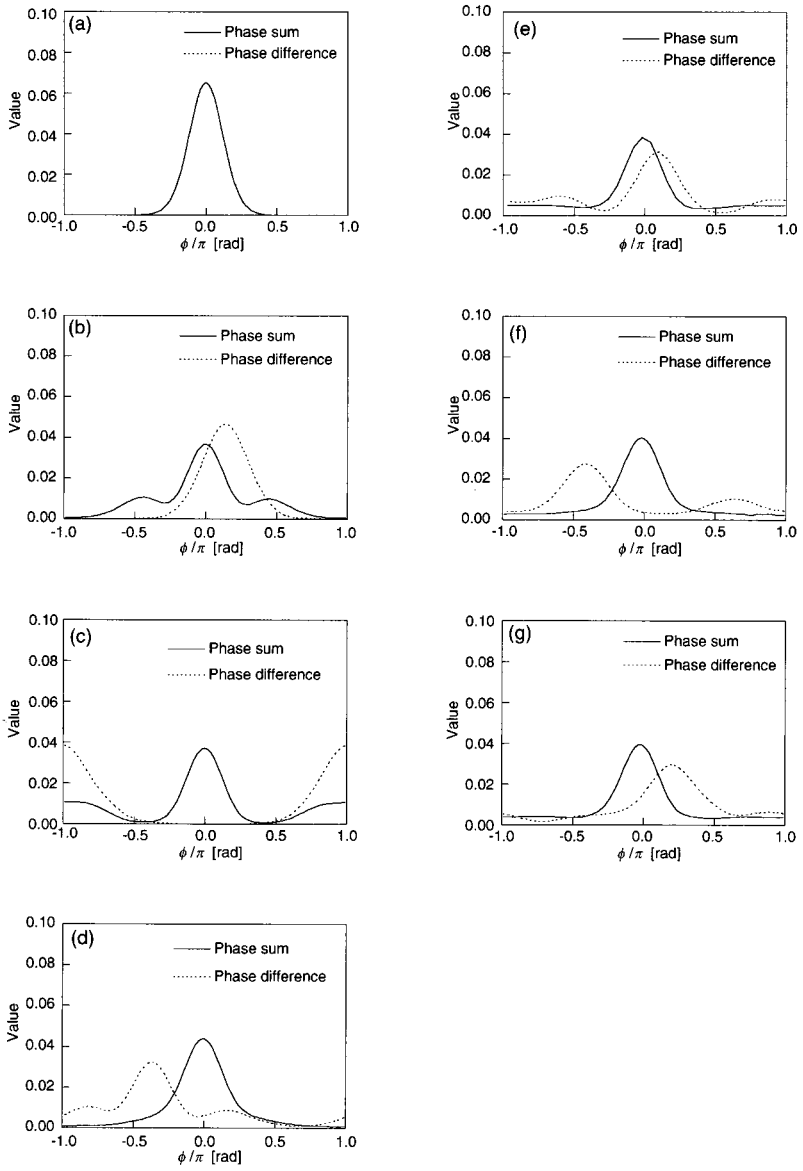

FIG. 4. Photon phase-sum (solid lines) and -difference (dotted lines) distributions of the two-mode coherent (TC) and two-mode squeezed coherent (TSC) fields at times (a)–(g) for (TC) and at times (a′)–(j′) for (TSC). These times are shown in Fig. 3. The distributions for the two-mode thermal field (TT) are not shown since it exhibits a uniform distribution with a constant value at an arbitrary time.

exhibits a single peak around $\pm\pi$, the distribution $P(\phi^+)$ is shown to be split into two peaks, one of which is around $\phi^+=0$ and the other is around $\phi^+=\pm\pi$. The phase difference between these two peaks is found to be about π, which corresponds to the situation of the $\pi/2$ difference between the side and main peaks observed in a one-mode field case [1,2]. Namely, it is predicted that the two-mode coherent field (TC) at time (c) hardly destroys the relative phase difference between the molecular states. This feature supports the fact that the region around time (c) for the two-mode coherent field (TC), is a quiescent region [1,2] (see Fig. 3 [TC-*dd*]). The first revival for the two-mode coherent field (TC) is shown to begin from around time (d), at which for the distribution $P(\phi^+)$ the split side peaks are shown to collide with the central peak around $\phi^+=0$ to become a somewhat broad single peak, while for the distribution $P(\phi^-)$ the split into three peaks is shown to begin. At time (e), the second collapse region, the distribution $P(\phi^-)$ for the two-mode coherent field (TC) evidently splits into three peaks in contrast to the distribution $P(\phi^+)$, which exhibits a nearly single peak. In the second revival region at time (f) for the two-mode coherent field (TC), the distribution $P(\phi^-)$ is characterized by two peaks, the larger one of which corresponds to the original central peak and the other (smaller one) is made by the collision between the split side peaks, while the distribution $P(\phi^+)$ maintains a single peak. Although the difference between the side and main peaks of the distribution $P(\phi^-)$ for the two-mode coherent field (TC) is found to be about π, the distribution is shown to be rather delocalized and some distributions exist between the two peaks. This result and the single peak of the distribution $P(\phi^+)$ for the two-mode coherent field (TC) at time (f) support the feature of the incipient stage of the second revival Rabi oscillations. In the revival region with larger amplitudes

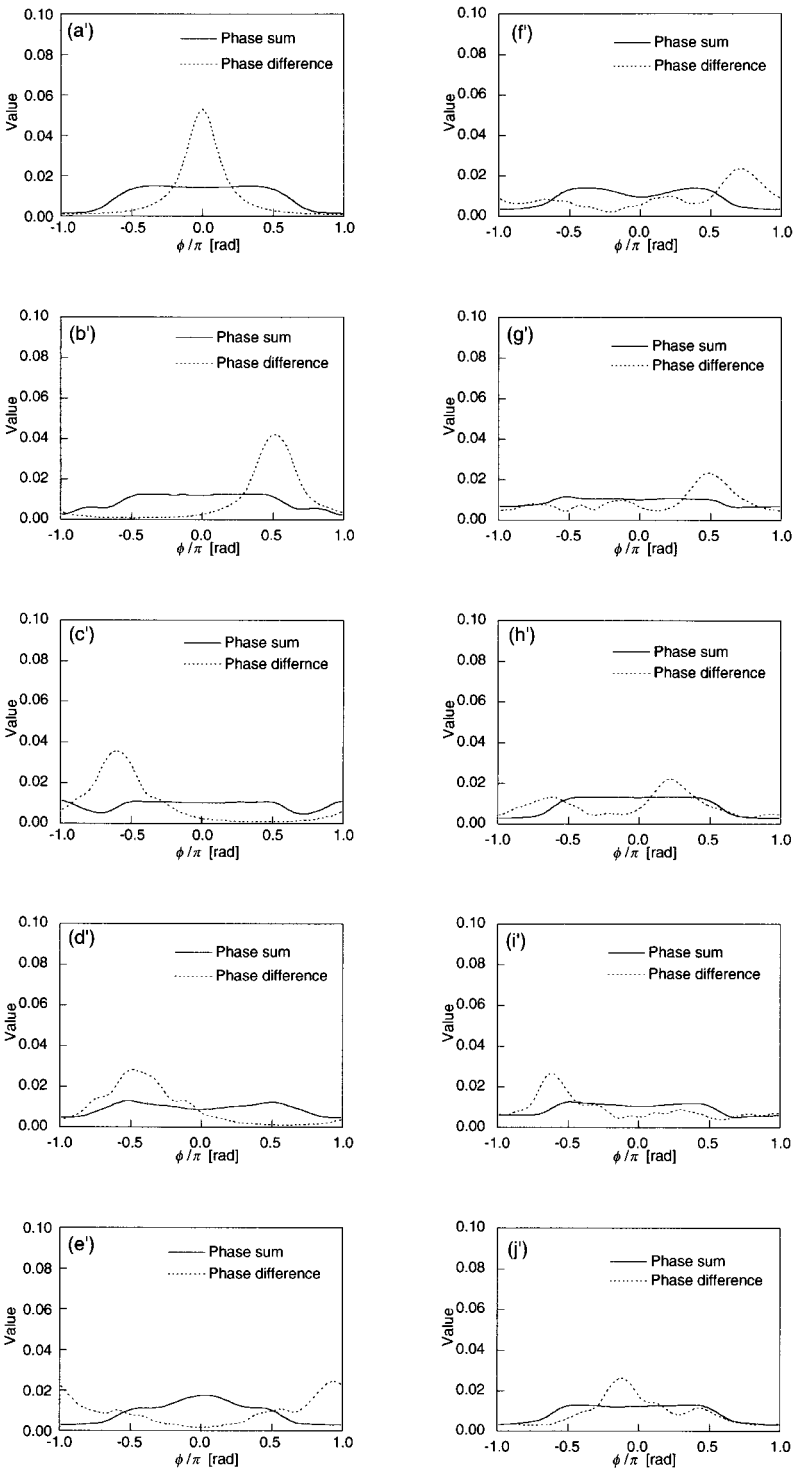

FIG. 4 (*Continued*).

of the Rabi oscillations for the two-mode coherent field (TC) at time (g), both the distributions $P(\phi^+)$ and $P(\phi^-)$ provide single peaks, which implies that each mode of the field possesses a fairly definite phase. These results indicate that the collapse-revival behavior of the molecular ground state under the two-mode coherent photon field (TC) corresponds to the splitting and colliding processes of both the distributions $P(\phi^+)$ and $P(\phi^-)$, i.e., two-mode phase distributions $P(\phi^1,\phi^2)$. If either phase state of $|\phi^+\rangle$ and $|\phi^-\rangle$ became an uncertainty state concerning its photon phase, the Rabi oscillations would be damped.

Second, we consider the two-mode squeezed coherent field (TSC) case. Although the molecular population dynamics for the two-mode squeezed coherent field (TSC) is simi-

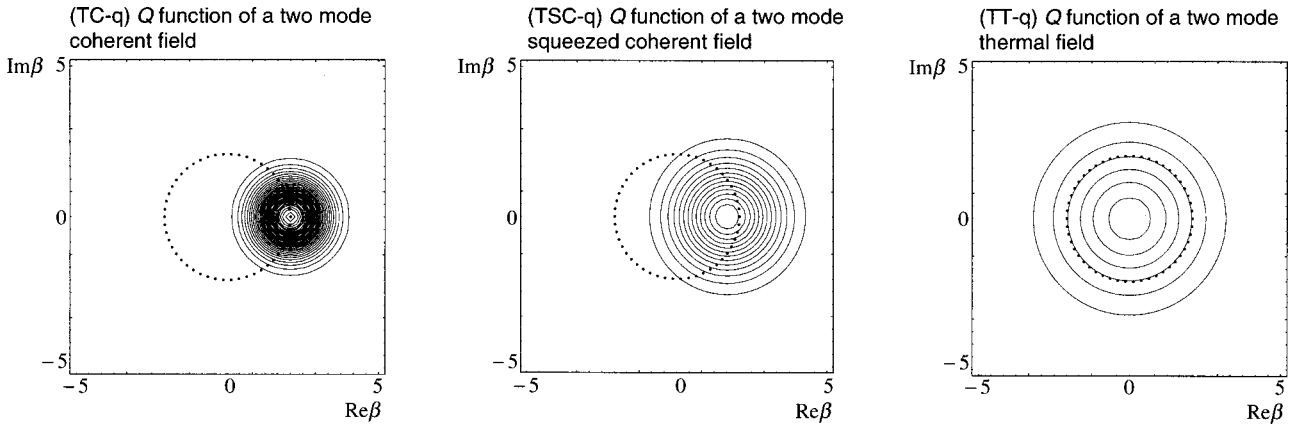

FIG. 5. One-mode Q function distributions in the complex β plane at the initial time for the two-mode coherent (TC), two-mode squeezed coherent (TSC), and two-mode thermal (TT) fields are shown in (TC-q), (TSC-q), and (TT-q), respectively. Contours with an interval 0.01 are drawn. The circle $|\beta| \equiv \sqrt{\langle \hat{n}_1 \rangle} (= \sqrt{\langle \hat{n}_2 \rangle})$ [$\sqrt{\langle \hat{n}_1 \rangle} (= \sqrt{\langle \hat{n}_2 \rangle})$: one-mode average photon number of the initial photon field] is also dotted in the contour plots.

lar to that for the two-mode coherent field (TC) (see Fig. 3 [(TC-*dd*) and (TSC-*dd*)]) the initial distributions $P(\phi^+)$ and $P(\phi^-)$ for the two-mode squeezed coherent field (TSC) are found to be different from those of the two-mode coherent field (TC) (see Fig. 4 [(TC)(a) and (TSC)(a′)]). In particular, it is shown that the initial distribution $P(\phi^+)$ of the two-mode squeezed coherent field (TSC) is remarkably broadened and approaches the uniform distribution observed in the thermal field. This feature supports the smaller contribution of two-photon processes to the collapse-revival behavior in the two-mode squeezed coherent field (TSC) case as compared with the two-mode coherent field (TC) case. It is found that in the first collapse region for the two-mode squeezed coherent field (TSC) at times (b′), (c′), and (d′) (see Fig. 3 [(TSC-*dd*]), although the distribution $P(\phi^+)$ splits into three peaks, their distinction is not clear and is nearly regarded as a uniform distribution. In contrast, it is shown that the distribution $P(\phi^-)$ of the two-mode squeezed coherent field (TSC) provides a fairly distinct single peak at the initial time and slowly splits into three peaks in the time region (b′)–(d′). This supports the slow collapse behavior in the time region (b′)–(d′) shown in Fig. 3 [(TSC-*dd*)]. At times (f′) and (g′), a relatively distinct single peak of the distribution $P(\phi^-)$ for the two-mode squeezed coherent field (TSC) appears, although the distribution $P(\phi^+)$ exhibits a broad peak like that for a thermal field, the feature of which supports the behavior in the first revival region (f′)–(g′) (see Fig. 3 [(TSC-*dd*)]). After time (g′), the degree of the splitting of the side peaks for the distribution $P(\phi^-)$ for the two-mode squeezed coherent field (TSC) is shown to be large, the feature of which supports the fact that the Rabi oscillations in the first revival-collapse region for (TSC) disappears after time (g′) (see Fig. 3 [(TSC-*dd*)]). Although the distribution $P(\phi^+)$ for the two-mode squeezed coherent field (TSC) at time (h′) exhibits a single broad peak and the distribution $P(\phi^-)$ is shown to be well split into two peaks with the phase difference π, the split two peaks of $P(\phi^-)$ are fairly delocalized and the some distributions exist in the intermediate phase region as compared with the two-mode coherent field (TC) case (see Fig. 4 [(TSC)(h′) and (TC)(f)]). As mentioned in the previous paragraph, this situation corresponds to the quiescent region or the incipient region of the second revival behavior shown in Fig. 3 [(TSC-*dd*)(h′)]. Further, the distribution $P(\phi^-)$ for the two-mode squeezed coherent field (TSC) is shown to become a single peak again going from time (i′) to (j′), although that is a fairly broad peak. Although this feature supports the enhancement of the amplitude of the Rabi oscillations of the second revival-collapse region, these oscillations are shown to be less dictinct than those of the two-mode coherent field (TC) case (see Fig. 3 [(TC-*dd*)(f)–(g) and (TSC-*dd*)(i′)–(j′)]), the feature of which is assumed to be caused by the indistinct colliding of the split phase distributions and the resultant broadness of the peak.

Third, we briefly explain the photon-phase distribution dynamics of the two-mode thermal field (TT) case. As mentioned above, the thermal field is a state with completely random phases, so that the two-mode photon-phase distribution is uniform (see Fig. 2 [(TT-2p)]). Namely, both the distributions $P(\phi^+)$ and $P(\phi^-)$ for the two-mode thermal field (TT) also provide uniform distributions with a constant value. These random phase components lead to a dynamical behavior of the molecular populations for the two-mode thermal field (TT) (shown in Fig. 3 [(TT-*dd*)]), in which the oscillations of the molecular populations are instantly damped and only the fluctuation remains at later times.

We here consider the differences in the feature of the collapse-revival behavior for these photon fields in view of their initial Q function distributions (Figs. 5 [(TC-q), (TSC-q), and (TT-q)]). The one-mode Q function distribution for the two-mode coherent field (TC) at the initial time is shown to be a single peak at $(|\beta_\lambda|, \phi_\lambda) = (2,0)$, while that for the two-mode thermal field (TT) is located at the origin and is much broader than that for the two-mode coherent field (TC). For the two-mode squeezed coherent field (TSC), the one-mode Q function distribution exhibits intermediate features between the two-mode coherent (TC) and the two-mode thermal (TT) fields: the Q function distribution of the two-mode squeezed coherent field (TSC) has a broad peak a

little sharper than that for the two-mode thermal field (TT) case, while the peak for the two-mode squeezed coherent field (TSC) is located at $|\beta_\lambda|$ ($\equiv\sqrt{\langle\hat{n}_\lambda\rangle-|\sinh r|^2}=\sqrt{4-|\sinh 1|^2}\approx 1.618\,302\,245$). It was found that the collapse and revival behavior corresponds to the splitting, the mutual counterrotating, and the colliding of the split distribution peaks of the Q function [1–5,42–44]. Since the dotted circle represents the same photon number (4) for a one-mode coherent field, the peak of the one-mode Q function distribution for the two-mode coherent field (TC) rotates along this dotted line. It is known for the two-mode thermal field (TT) that the Q function distribution located at the origin is unsplit and only its peak intensity is changed, the behavior of which corresponds to a change in the average photon number [5]. The uniform phase distribution of the thermal field indicates that it contains all photon number states randomly phased with respect to each other. Since the Q function distribution for a coherent field with a larger number of photons needs longer time to split, the distribution in the inner region is predicted to rotate faster than that in the outer region [50]. This indicates that the Q function distribution for the two-mode squeezed coherent field (TSC) possesses both faster and slower rotating components as compared to the two-mode coherent field (TC) case. This feature supports the enhancement of the first collapse region, the earlier start of the first revival, and the fewer differences between the amplitudes of the first and second revival-collapse oscillations in the case of the two-mode squeezed coherent field (TSC) (see Fig. 3).

D. Dynamics of the off-diagonal molecular density matrix

Figure 6 shows the time evolution of the magnitude of off-diagonal molecular density matrix elements $|\rho_{1,2}^{\mathrm{mol}}|$, $|\rho_{2,3}^{\mathrm{mol}}|$, and $|\rho_{1,3}^{\mathrm{mol}}|$ for these three types of two-mode photon fields. The magnitude of the off-diagonal molecular density ($|\rho_{i,j}^{\mathrm{mol}}|$) represents the degree of the coherency (the definite relative phase) between the states (i and j) of a molecule. From a comparison among the off-diagonal densities for the two-mode coherent (TC) and two-mode squeezed coherent (TSC) fields, for the two-mode coherent field (TC) the $|\rho_{1,3}^{\mathrm{mol}}|$ is found to be much larger than $|\rho_{1,2}^{\mathrm{mol}}|$ and $|\rho_{2,3}^{\mathrm{mol}}|$, while for the two-mode squeezed coherent field (TSC) they are shown to provide similar average values. This remarkable difference in $|\rho_{1,3}^{\mathrm{mol}}|$ between the two-mode coherent (TC) and two-mode squeezed coherent (TSC) fields is attributed to the difference in the distributions $P(\phi^+)$ between these two fields: the distribution $P(\phi^+)$ for the two-mode squeezed coherent field (TSC) is found to be much broader than that for the two-mode coherent field (TC) although the distributions $P(\phi^-)$ for both these fields are shown to provide similar single peaks. Namely, the coherence between molecular states 1 and 3 for the two-mode squeezed coherent field (TSC) is considered to be damped by the broader distribution of $P(\phi^+)$ for (TSC), which has a resonant frequency with energy interval E_{31}. The dynamical behavior of $|\rho_{1,3}^{\mathrm{mol}}|$ is also found to be related to that of the distribution $P(\phi^+)$. For the two-mode coherent field (TC), the increase in $|\rho_{1,3}^{\mathrm{mol}}|$ from

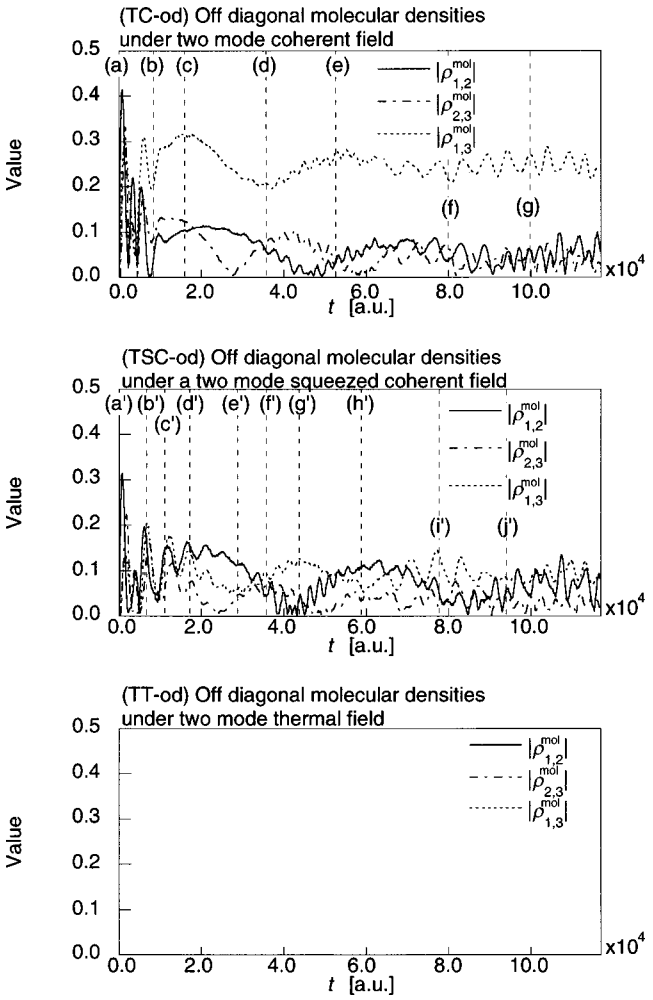

FIG. 6. Time evolution of the magnitude of the off-diagonal molecular densities $|\rho_{1,2}^{\mathrm{mol}}|$, $|\rho_{2,3}^{\mathrm{mol}}|$, and $|\rho_{1,3}^{\mathrm{mol}}|$, for the two-mode coherent (TC), two-mode squeezed coherent (TSC), and two-mode thermal (TT) fields is shown in (TC-*od*), (TSC-*od*), and (TT-*od*), respectively.

time (b) to (c) corresponds to the displacement of the split side peaks of the distributions $P(\phi^+)$ from about $\pm\pi/2$ to $\pm\pi$ (see Fig. 4 [(TC)]), which corresponds to the situation of split peaks on $\pm\pi/2$ for the one-mode field case. This situation decreases the ability of the destruction of the relative phase between molecular states and then enhances the coherence between molecular states 1 and 3. On the other hand, the decrease in $|\rho_{1,3}^{\mathrm{mol}}|$ for the two-mode coherent field (TC) from time (c) to (d) corresponds to the disappearance of the peaks on $\pm\pi$ and the generation of a broader peak of the distribution $P(\phi^+)$. At later times [after time (e)], the distributions $P(\phi^+)$ for the two-mode coherent field (TC) are found to almost maintain their shapes (a single peak). This leads to the fact that the large $|\rho_{1,3}^{\mathrm{mol}}|$ values with only small oscillations are observed at later times [after time (e)] for the two-mode coherent field (TC) (see Fig. 6 [(TC-*od*)]). Even in the case of the two-mode squeezed coherent field (TSC), the variation in $|\rho_{1,3}^{\mathrm{mol}}|$ is found to be associated with that of the splitting and colliding behavior of the distributions $P(\phi^+)$. However, it is found that the magnitude and width of the

distribution $P(\phi^+)$ for the two-mode squeezed coherent field (TSC) is much smaller and much broader than those for the two-mode coherent field (TC), respectively, so that the $|\rho_{1,3}^{\mathrm{mol}}|$ for the two-mode squeezed coherent field (TSC) exhibits a more indistinct variation with a much smaller magnitude as compared to the two-mode coherent field (TC) case.

For the two-mode thermal field (TT) case, all the off-diagonal molecular densities are shown to vanish, the feature of which is reasonable by considering that the random-phase components of the thermal field completely destroy the relative-phase relation between molecular states.

E. Molecular entropy dynamics

The molecular entropy S^{mol} represents the degree of the correlation between the molecule and two-mode photon field. Since the two modes (modes 1 and 2) of the field are resonant with energy intervals E_{21} and E_{32} of the molecule, respectively, the variation in S^{mol} is predicted to be associated with that in the off-diagonal molecular density $|\rho_{1,3}^{\mathrm{mol}}|$. Actually, for the two-mode coherent field (TC) case, the variation in $|\rho_{1,3}^{\mathrm{mol}}|$ from time (b) to (e) (Fig. 6 [(TC-*od*)]) is found to be just the reverse of the S^{mol} from time (b) to (e) (Fig. 7 [(TC-*s*)]). This is evident from the following relation. S^{mol} increases with increasing the correlation between the two-mode photon field and the molecule. In that region, the phase uncertainty in the photon field destroys the relative phase (coherence) between the molecular states. This leads to a decrease in $|\rho_{1,3}^{\mathrm{mol}}|$. Such a relation is also observed in the two-mode squeezed coherent field (see Fig. 6 [(TSC-*od*)] and Fig. 7 [(TSC-*s*)]), while the significant decrease in S^{mol} in the early time region (c)–(d), i.e., the quiescent region, for the two-mode coherent field (TC) case is not found in the case of the two-mode squeezed coherent field (TSC). Such an attractive decrease in S^{mol}, i.e., the correlation between molecules and photons, is important for the generation of the optical "Schrödinger cat state" [12] in the case of the one-mode photon field. For the two-mode thermal field (TT) case, the S^{mol} increases quickly to the maximum value and remains fluctuating with small oscillations thereafter. This reflects the fact that the thermal field quickly destroys the coherency between the molecular states. In view of the significant decrease in S^{mol}, the dynamical feature of the two-mode squeezed coherent field (TSC) case is found to rather resemble that of the two-mode thermal field (TT) case as compared with the two-mode coherent field (TC) case, although there are found to be many similar features concerning other properties, e.g., collapse and revival behavior (Fig. 3) and the nonzero off-diagonal densities (Fig. 6).

V. CONCLUSION

We investigated the dynamics of a three-state molecular model interacting with uncorrelated and correlated photon fields, i.e., two-mode coherent, two-mode thermal, and two-mode squeezed coherent fields. We showed that the two-mode squeezed coherent field exhibits a similar collapse-revival behavior of the Rabi oscillations to that of the two-mode coherent field, although the one-mode photon-number

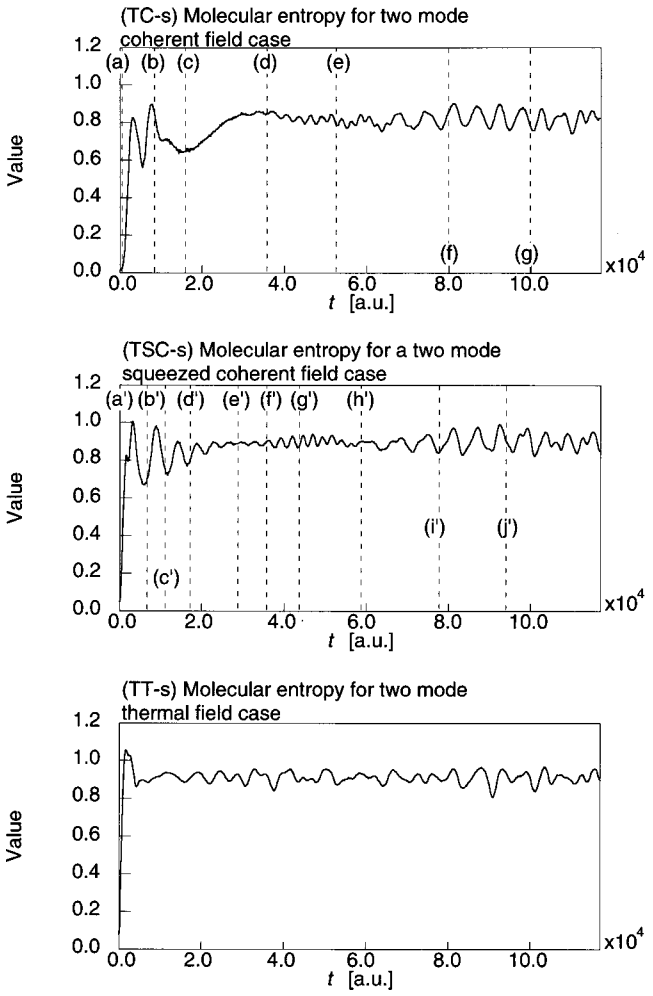

FIG. 7. Time evolution of the molecular entropies (S^{mol}) for the two-mode coherent (TC), two-mode squeezed coherent (TSC), and two-mode thermal (TT) fields is shown in (TC-*s*), (TSC-*s*), and (TT-*s*), respectively.

and -phase distributions possess intermediate features between the two-mode coherent and two-mode thermal fields. Such collapse-revival behavior was found to be associated with the splitting and colliding behaviors of the two-mode photon-phase distributions, e.g., phase-sum and -difference distributions. On the other hand, the magnitude of the off-diagonal molecular density matrix element ($|\rho_{1,3}^{\mathrm{mol}}|$) between states 1 and 3 for the two-mode squeezed coherent field case were found to be much smaller than that for the two-mode coherent field although other elements ($|\rho_{1,2}^{\mathrm{mol}}|$ and $|\rho_{2,3}^{\mathrm{mol}}|$) for the two-mode squeezed coherent field exhibit similar behavior to those for the two-mode coherent field. The off-diagonal molecular densities for the two-mode coherent and two-mode squeezed coherent fields are also found to be different from those of the two-mode thermal fields, in which these elements vanish. We attributed these features to the differences in the two-mode photon-phase distributions among these fields: the initial phase-sum distribution for the two-mode squeezed coherent field exhibits a much broader peak (like a uniform distribution observed in the thermal field) than that for the two-mode coherent field (which has a single sharp peak), and the two-mode phase

distributions for the two-mode thermal field are uniform. The differences in the off-diagonal molecular densities are also reflected in the dynamical behavior of the molecular entropy (S^{mol}), which represents the degree of correlation between the molecule and photons. For example, a significant decrease in S^{mol} in the early-time region for the two-mode coherent field case is not observed in the case of the two-mode squeezed coherent field. Judging from the present results, the two-mode squeezed coherent field with an intermediate squeezing intensity between that for the two-mode coherent field and that for the two-mode squeezed vacuum field exhibits a somewhat similar collapse-revival behavior of the Rabi oscillations to that for the two-mode coherent field, while the two-mode squeezed coherent field provides significantly different features in the photon-phase sum, the off-diagonal molecular densities $|\rho_{1,3}^{\mathrm{mol}}|$, and the correlation between the molecule and the two-mode photons, as compared to the two-mode coherent field. In conclusion, the two-mode squeezed coherent fields are predicted to directly provide remarkable effects on the coherence between the molecular states and on the molecule-photon correlation by changing the squeezing parameters. Such attractive features will contribute to the investigation of quantum dynamical phenomena in molecular science in the future.

ACKNOWLEDGMENTS

This work was supported by a Grant-in-Aid for Scientific Research (Nos. 12042248, 12740320, and 10149105) from the Ministry of Education, Culture, Sports, Science and Technology, Japan.

[1] M. Nakano and K. Yamaguchi, Chem. Phys. Lett. **295**, 317 (1998).
[2] M. Nakano and K. Yamaguchi, Chem. Phys. **252**, 115 (2000).
[3] M. Nakano and K. Yamaguchi, Chem. Phys. Lett. **304**, 241 (1999).
[4] M. Nakano and K. Yamaguchi, J. Phys. Chem. **103**, 6036 (1999).
[5] M. Nakano and K. Yamaguchi, J. Chem. Phys. **112**, 2769 (2000).
[6] M. Nakano and K. Yamaguchi, Chem. Phys. Lett. **324**, 289 (2000).
[7] M. Nakano and K. Yamaguchi, Chem. Phys. Lett. **317**, 103 (2000).
[8] E. T. Jaynes and F. W. Cummings, Proc. IEEE **51**, 100 (1963).
[9] L. Allen and J. H. Eberly, *Optical Resonance and Two-Level Atoms* (Wiley, New York, 1975).
[10] P. L. Knight and P. W. Milonni, Phys. Rep. **66**, 21 (1980).
[11] P. W. Milonni and S. Singh, Adv. At., Mol., Opt. Phys. **28**, 75 (1990).
[12] B. W. Shore and P. L. Knight, J. Mod. Opt. **40**, 1195 (1993).
[13] J. H. Eberly, N. B. Narozhny, and J. J. Sanchez-Mondragon, Phys. Rev. Lett. **44**, 1323 (1980).
[14] N. B. Narozhny, J. J. Sanchez-Mondragon, and J. H. Eberly, Phys. Rev. A **23**, 236 (1981).
[15] P. L. Knight and P. M. Radmore, Phys. Rev. A **26**, 676 (1982).
[16] F. T. Hioe, J. Math. Phys. **23**, 2430 (1982).
[17] R. R. Puri and G. S. Agarwal, Phys. Rev. A **33**, 3610 (1986).
[18] I. Sh. Averbukh, Phys. Rev. A **46**, R2205 (1992).
[19] P. F. Góra and C. Jedrzejek, Phys. Rev. A **48**, 3291 (1993).
[20] P. F. Góra and C. Jedrzejek, Phys. Rev. A **49**, 3046 (1994).
[21] M. Brune, F. Schmidt-Kaler, A. Maali, J. Dreyer, E. Hagley, J. M. Raimond, and S. Haroche, Phys. Rev. Lett. **76**, 1800 (1996).
[22] J. A. Yeazell, M. Mallalieu, and C. R. Stroud Jr., Phys. Rev. Lett. **64**, 2007 (1990).
[23] A. N. Chaba, M. J. Collet, and D. F. Wall, Phys. Rev. A **46**, 1499 (1992).
[24] J. I. Cirac, R. Blatt, A. S. Parkins, and P. Zoller, Phys. Rev. Lett. **70**, 556 (1993); Phys. Rev. A **49**, 1202 (1994).
[25] *The Physics of Quantum Information: Quantum Cryptography, Quantum Teleportation, Quantum Computation*, edited by D. Bouwmeester, A. Ekert, and A. Zeilinger (Springer-Verlag, Berlin, 2000).
[26] W. K. Laí, V. Buzek, and P. L. Knight, Phys. Rev. A **44**, 6043 (1991).
[27] V. Buzek and T. Quang, J. Opt. Soc. Am. B **6**, 2447 (1989).
[28] R. Loudon and P. L. Knight, J. Mod. Opt. **34**, 709 (1987).
[29] S. M. Barnett and P. L. Knight, J. Opt. Soc. Am. B **2**, 467 (1985).
[30] Y. Takahashi and H. Umezawa, Collect. Phenom. **2**, 55 (1975).
[31] W. Israel, Phys. Lett. **57A**, 107 (1976); H. Umezawa, A. E. I. Johansson, and Y. Yamanaka, Class. Quantum Grav. **7**, 385 (1990); R. Laflamme, Physica A **158**, 58 (1989).
[32] A. K. Ekert and P. L. Knight, Am. J. Phys. **57**, 692 (1989).
[33] C. M. Caves and B. L. Schumaker, Phys. Rev. A **31**, 3068 (1985).
[34] B. L. Schumaker and C. M. Caves, Phys. Rev. A **31**, 3093 (1985).
[35] C. T. Lee, Phys. Rev. A **42**, 4193 (1990).
[36] C. M. Caves, C. Zhu, G. J. Milburn, and W. Schleich, Phys. Rev. A **43**, 3854 (1991).
[37] M. Selvadoray, M. Sanjary Kumar, and R. Simon, Phys. Rev. A **49**, 4957 (1994).
[38] D. T. Pegg and S. M. Barnett, Phys. Rev. A **39**, 1665 (1989).
[39] R. Lynch, Phys. Rep. **256**, 367 (1995).
[40] S. M. Barnett and D. T. Pegg, J. Mod. Opt. **44**, 225 (1997).
[41] S. M. Barnett and D. T. Pegg, Phys. Rev. A **42**, 6713 (1990).
[42] J. Eiselt and H. Risken, Phys. Rev. A **43**, 346 (1991).
[43] M. J. Werner and H. Risken, Phys. Rev. A **44**, 4623 (1991).
[44] C. A. Miller, J. Hilsenbeck, and H. Risken, Phys. Rev. A **46**, 4323 (1992).
[45] P. K. Aravind and J. O. Hirschfelder, J. Phys. Chem. **88**, 4788 (1984).
[46] A. Wehrl, Rev. Mod. Phys. **50**, 221 (1978).
[47] P. A. M. Dirac, Proc. R. Soc. London, Ser. A **114**, 243 (1927).
[48] L. Susskind and J. Glogower, Physica (Amsterdam) **1**, 49 (1964).
[49] Z. G. Soos and S. Ramasesha, J. Chem. Phys. **90**, 1067 (1989).
[50] G. MIlburn, Opt. Acta **31**, 671 (1984).